ECS Journal of Solid State Science and Technology, **6** (4) M19-M23 (2017)
2162-8769/2017/6(4)/M19/5/$37.00 © The Electrochemical Society

Fullerene Mediated Electrosynthesis of Au/C_{60} Nanocomposite

Vitaliy V. Yanilkin,[a,z] Natalya V. Nastapova,[a] Gulnaz R. Nasretdinova,[a] Yuri N. Osin,[b] and Aidar T. Gubaidullin[a]

[a]*A. E. Arbuzov Institute of Organic and Physical Chemistry, Kazan Scientific Center, Russian Academy of Sciences, 420088 Kazan, Russia*
[b]*Kazan Federal University, Interdisciplinary Center "Analytical Microscopy", 420018 Kazan, Russia*

C_{60} fullerene mediated electroreduction of Au(I) at potentials of the $C_{60}/C_{60}^{\bullet-}$ redox couple was used to perform the electrosynthesis of an AuNP/C_{60} nanocomposite in DCB-DMF (2:1)/0.1 M Bu_4NCl medium. The nanocomposite consists of separate gold nanoparticles with various shapes and a mean size of ~27 ± 14 nm, as well as larger nanoaggregates of such particles, isolated in a fullerene matrix. The mean size of metal crystallites is 9–14 nm. The electrolysis occurs efficiently, and Au(I) is quantitatively reduced to Au(0) upon consumption of the theoretical amount of electricity. The resulting metal nanoparticles and the nanocomposite are not deposited on the electrode and are completely stabilized in the solution bulk. All the particles were characterized by electron microscopy methods (SEM, HR TEM) and X-ray powder diffraction (XRPD).

Manuscript submitted December 9, 2016; revised manuscript received January 12, 2017. Published January 19, 2017.

Fullerenes are new objects that have attracted general attention of researchers at the turn of the 21th century. From electrochemical point of view, they are primarily attractive as they can accept up to six electrons per molecule in a stepwise and reversible manner to give stable mono- and multianions.[1–5] The anionic reduction products of numerous fullerene derivatives, in particular, those of many methanofullerenes and fulleropyrrolidines,[6] are also rather stable. The reversibility of electron transfer stages makes it possible to use fullerenes and their derivatives as mediators in the transfer of one or more electrons from an electrode to a substrate. Anion radicals and dianions of fullerenes and their derivatives are not protonated with such proton donors as water or phenol.[6–10] Hence, fullerenes and their derivatives can serve as mediators at potentials of generation of these anionic particles not only in aprotic media but also in moderate proton-donating ones. This considerably expands the scope of their applicability as mediators. However, in reality, the synthetic potential of fullerenes in this role has been revealed quite incompletely, and only a few studies are available on the mediator properties of C_n fullerenes at potentials of generation of $C_n^{\bullet-}$ anion radicals, C_n^{2-} dianions, and $C_n^{\bullet 3-}$ radical trianions in electroreduction of organic compounds,[11–25] oxygen,[26] and nitrite ions.[27]

In recent years, metal nanoparticles (MNP) have been attracting a growing interest due to their unique properties and diverse uses in catalysis, electronics, biomedicine, optics, analysis, etc.[28–34] Mediated electrosynthesis[35–47] involving mediated electroreduction of metal complexes and ions in solution is an efficient method for MNP electrosynthesis in solution bulk. Unlike the other known electrochemical methods, such as pulsed sonoelectrochemistry[48–50] and the Reetz method,[51–55] in this method the stage of reduction of metal ions was moved from the electrode surface to the solution bulk. In this case, the mediator is reduced on the cathode; the reduced form of the mediator diffuses into the solution bulk where it reduces a metal ion or complex. Thus, deposition of the metal, which is the main factor that restricts the use of electrochemistry in MNP synthesis, is excluded completely or minimized.

The method capability and efficiency was recently demonstrated by the syntheses of Pd,[35–40] Ag,[41–45] Co,[46] Au[47] nanoparticles in the absence and in the presence of NP stabilizers in aqueous, aqueous-organic and non-aqueous media, using salts and complexes of the metals or with in situ generation of metal ions in solution by dissolution of the anode metal during the electrolysis. The method is equally efficient both with soluble ions and complexes ($[PdCl_4]^{2-}$, Ag^+, AuCl, $[CoCl_4]^{2-}$) and with poorly soluble metal salts (AgCl, spherical nanoparticles of $[PdCl_4]^{2-}$@CTAC), irrespective of whether the mediator is more easily reduced on the electrode than the metal substrate. The NPs obtained were stabilized by tetraviologen calixresorcines, incapsulation of polymeric spherical NPs in nanocapsules, in polyvinylpyrrolidone or cetyltrimethylammonium (CTAC) shell, and by binding aminoalkylated silicate NPs on a surface. Methylviologen[36–45,47] and tetraviologen calix[4]resorcines,[35–38,42,43] as well as anthracene[46] and molecular oxygen,[47] were mostly used as the mediators.

In this paper we report that a new application of fullerenes as a mediator is possible, namely, fullerene C_{60} can be used in the electrochemical reduction of Au(I) in *o*-dichlorobenzene/N,N-dimethylformamide medium (2:1) containing 0.1 M Bu_4NCl as the supporting electrolyte, as well as in the fullerene mediated electrosynthesis of the Au-NP/C_{60} nanocomposite material. The use of fullerenes and their derivatives as mediators in the electrosynthesis of metal nanoparticles was not reported before.

Experimental

The study was performed using cyclic voltammetry (CV), preparative electrolysis, scanning electron microscopy (SEM), high resolution transmission electron microscopy (HR TEM), powder X-ray diffraction (XRPD) and UV and visible spectroscopy.

Reagents.—Gold Chloride (Alfa Aesar), fullerene (C_{60}), Bu_4NCl (Fluka), N,N-dimethylformamide (DMF) (Alfa Aesar), and 1,2-dichlorobenzene (*o*-DCB) (Alfa Aesar) were used without additional purification.

Cyclic voltammograms.—(CV curves) were recorded using a P-30J potentiostat (without IR compensation) in an argon atmosphere in an *o*-dichlorobenzene/N,N-dimethylformamide (2:1) medium with 0.1 M Bu_4NCl as the supporting electrolyte. A glassy carbon disc electrode (dia. 2.0 mm) sealed into a glass tube was used as the working electrode. Prior to each measurement, the electrode was mechanically polished. Platinum wire was used as the auxiliary electrode. Potentials were measured and reported versus an aqueous saturated calomel electrode (SCE) connected to the solution being studied through a bridge containing the supporting electrolyte and having a potential of −0.57 V relative to formal potential $E_0{}'\ Fc^{+/0}$ (internal standard). The temperature was 295 K. The diffusion nature of the peak currents i_p was proven using the theoretical shape of the voltammogram and the linear dependence i_p - $\nu^{1/2}$ by varying the potential scan rate ν from 10 to 200 mV/s.

Preparative electrolysis was carried out in a three-electrode glass cell equipped with a diaphragm (porous glass), in potentiostatic mode (−0.40 V vs. SCE), in argon atmosphere at room temperature (T = 295 K) using a P-30J potentiostat. The solution was stirred with a magnetic stirrer during the electrolysis. A GC plate (S = 5.6 cm^2) was used as the working electrode and an SCE was used as the reference electrode. The latter was connected with the solution being studied

[z]E-mail: yanilkin@iopc.ru

through a bridge containing the reference electrolyte. A platinum wire immersed in the supporting electrolyte solution was used as the auxiliary electrode. A working solution (23 ml) for the electrolysis was prepared by dissolving 21.6 mg C_{60} (1.3 mM), 5.2 mg AuCl (1.0 mM) and 417 mg of the supporting electrolyte Bu_4NCl (0.1 M) in an *o*-dichlorobenzene/N,N-dimethylformamide mixture (2:1).

After completion of the electrolysis, the resulting solution was studied by CV on a GC indicator electrode (dia. 2.0 mm).

To study the nanoparticles obtained in the electrolysis by SEM, HR TEM and XRPD, the solvent was removed in vacuo from the solution, while the deposit was dispersed in water by sonication and reprecipitated by centrifugation (15 000 rpm, 1 h). Using a similar method, the resulting precipitate was twice washed with toluene and then twice washed with ethanol. Prior to SEM, HR TEM and XRPD, the suspension was dispersed in ethanol by sonication. In the case of SEM, the resulting solution was applied onto a titanium foil surface preliminarily cleaned by ultrasonic treatment in water and in acetone. After that, the sample was dried in air with slight heating (up to 40°C). In the case of HR TEM, 10 μl of the sample suspension was placed on a 3 mm copper mesh with formvar/carbon support and dried at room temperature. After complete drying, the mesh in a special graphite holder was placed into a transmission electron microscope in order to perform the microanalysis.

Electron microscopic analysis.—The morphology of the sample surface was studied using a Merlin high-resolution scanning electron microscope (Carl Zeiss) equipped with ASB, SE and STEM detectors. Elementary analyses were carried out using an EDS AZTEC X-MAX detector from Oxford Instruments combined with the microscope. HR TEM analysis of samples was carried out using a Hitachi HT7700 Excellence transmission electron microscope. The examination was carried out at accelerating voltages of 80–100 kV in TEM mode.

X-ray powder diffraction (XRPD).—measurements were performed on a Bruker D8 Advance diffractometer equipped with a Vario attachment and Vantec linear PSD, using Cu radiation (40 kV, 40 mA) monochromated by a curved Johansson monochromator (λ Cu $K_{\alpha 1}$ 1.5406 Å). Room-temperature data were collected in the reflection mode with a flat-plate sample. Sample was applied in liquid form on the surface of a standard zero diffraction silicon plate. After drying the layer, a few more layers were applied on top of it to increase the total amount of the sample. The sample was kept spinning (15 rpm) throughout the data collection. Patterns were recorded in the 2Θ range between 3° and 105°, in 0.008° steps, with a step time of 0.1–5.0s. Several diffraction patterns in various experimental modes were collected for the sample. Processing of the data obtained was performed using EVA[56] and TOPAS [TOPAS V3: General profile and structure analysis software for powder diffraction data. (2005). Technical Reference. Bruker AXS. Karlsruhe. Germany.- 117 p] software packages. The PDF-2 powder X-ray diffraction database (ICDD PDF-2, Release 2005–2009) was used to identify the crystalline phase.

UV and visible spectra were recorded on a Perkin-Elmer Lambda 25 spectrometer.

Results and Discussion

Cyclic voltammetry.—The CV curve of 1.0 mM Au(I) (AuCl or $[AuCl_2]^-$)[47] recorded on a GC electrode in DCB-DMF (2:1)/0.1 M Bu_4NCl medium shows one irreversible diffusion-limited reduction peak (the C_1 peak, Figure 1) ($E_{C1} = -0.03$ V vs. SCE). The oxidation peak of metallic gold generated and deposited on the electrode, which is observed in aqueous media at a potential of $E_p^{A1} = +0.92$ V[47], cannot be recorded here due to oxidation of the supporting electrolyte in this potential range. Four diffusion reversible reduction peaks of C_{60} fullerene (1.3 mM) are recorded under similar conditions (the C_2, C_3, C_4, and C_5 peaks, Figure 1) at more negative potentials ($E_{C2} = -0.38$ V, $E_{C3} = -0.82$ V, $E_{C4} = -1.36$ V, $E_{C5} = -1.87$ V), in full agreement with literature data.[6,10]

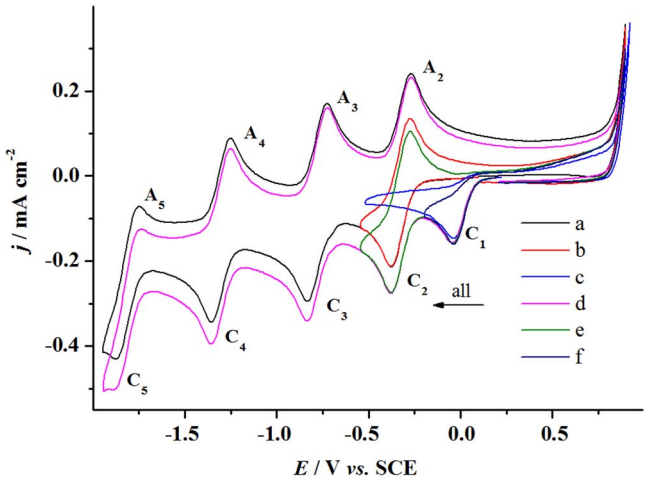

Figure 1. CV curves of 1.3 mM C_{60} (a, b), 1.0 mM AuCl (c) and 1.3 mM C_{60} + 1.0 mM AuCl (d-f) in DCB-DMF (2:1)/0.1 M Bu_4NCl medium. $\nu = 100$ mV/s.

All the parameters of the CV curve for the Au(I) (1.0 mM) + C_{60} (1.3 mM) system match those of the additive curve of both components taken separately, irrespective of the reversal potential (Figure 1). Hence, no noticeable binding of Au(I) and the generated Au(0) particles by the fullerene occurs on the electrode surface or in the near-electrode space. Au(I) particles are not bound with fullerene in the solution bulk, either, as indicated by the full match of fullerene absorption spectra in the visible region in the presence and in the absence of AuCl in the solution (Figure 2).

With an increase in the time of preliminary electrode exposure at the Au(I) reduction potential (E = −0.10 V) (Figure 3a), the height of the reduction peak of the metal ion decreases somewhat due to the depletion of the near-electrode layer in Au(I) during the microelectrolysis and the irreversibility of its reduction. This decrease is more pronounced if microelectrolysis is performed at the potential of the first step of C_{60} reduction (E = −0.40 V) (Figure 3b), whereas the heights of the fullerene peaks C_2, C_3 and A_2 remain unchanged. These data mean that the $C_{60}^{\bullet -}$ anion radicals are quite stable for at least three minutes under the experimental conditions, are reoxidized to C_{60} in the CV mode used, are not adsorbed on the electrode, and

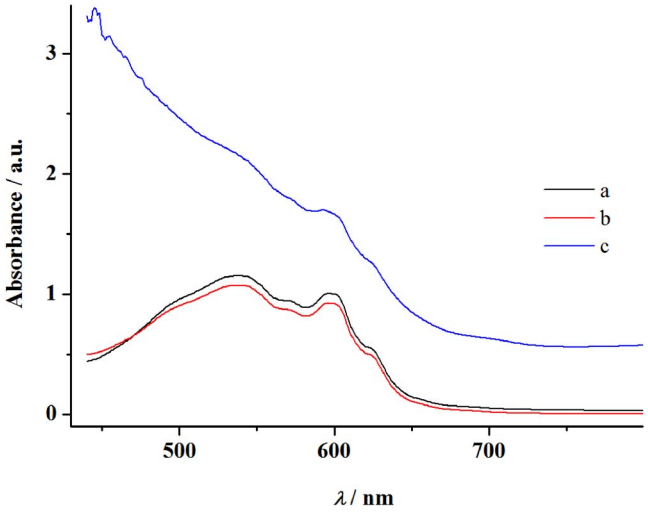

Figure 2. Absorption spectrum of solutions: 1.3 mM C_{60} (a), 1.3 mM C_{60} + 1.0 mM AuCl before (b) and after the electrolysis at −0.4 V (Q = 1.0 F as calculated with respect to AuCl) (c) in the DCB-DMF (2:1)/0.1 M Bu_4NCl medium.

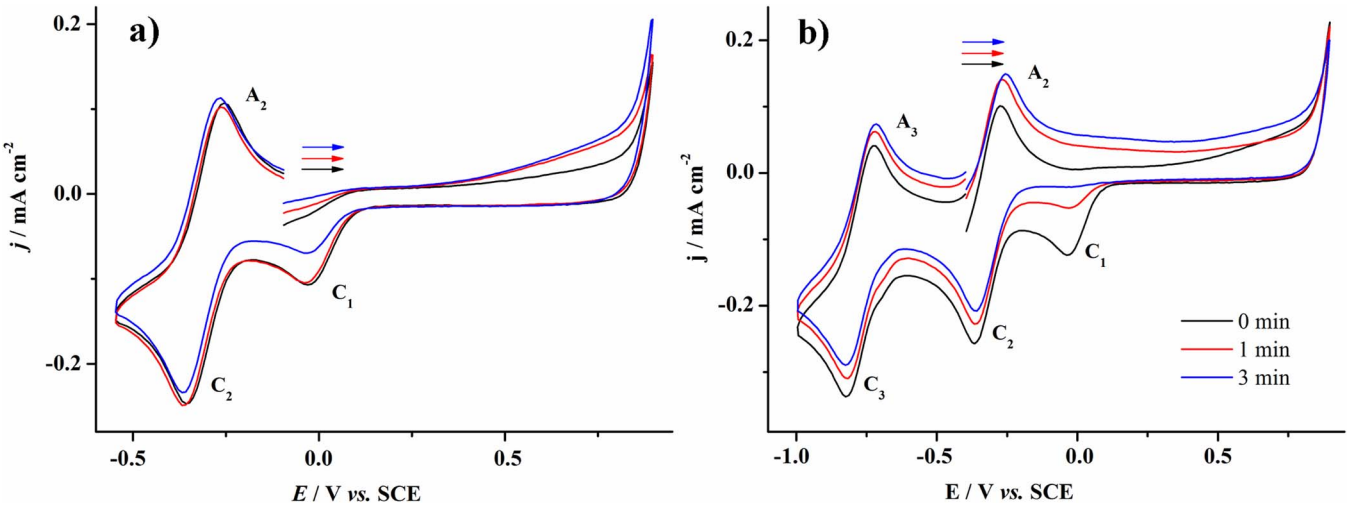

Figure 3. CV curves of the 1.3 mM C_{60} + 1.0 mM AuCl system after exposing the electrode at potentials of −0.10 V (a) and −0.40 V (b) for various period. $\nu = 100$ mV/s.

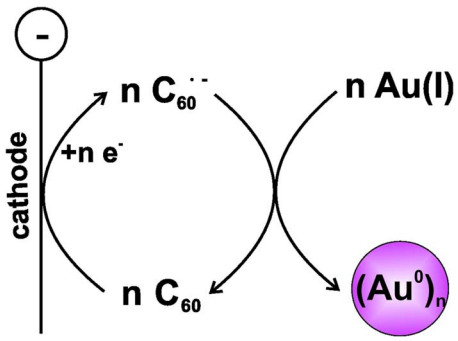

Scheme 1. Fullerene mediated Au(I) reduction.

homogeneously reduce Au(I) in the near-electrode solution layer. In other words, mediated Au(I) reduction occurs at potentials of the first reduction peak of C_{60} (Scheme 1).

Preparative electrosynthesis.—Based on the voltammetry data obtained, we performed a preparative electroreduction of this system Au(I) (1.0 mM) + C_{60} (1.3 mM) in the DCB-DMF (2:1)/0.1 M Bu_4NCl medium in a diaphragm electrolyzer at controlled potential of the first fullerene reduction peak (E = −0.40 V). The current decreased from 2.5 mA to 1.5 mA during the electrolysis. 1.0 F of electricity with respect to Au(I) was passed. The homogeneous solution was initially purple (the color of fullerene). The color changed during the electrolysis and became dark-brown at the end of the electrolysis (Figure 4). The mass of the cathode did not change during the electrolysis. After the end of the electrolysis, the Au(I) reduction peak on the CV curve is absent and only reversible C_{60} reduction and reoxidation peaks are recorded, with intensities just slightly lower than those for the fullerene taken separately (Figure 5). Hence, upon passage of the theoretical amount of electricity, Au(I) is reduced quantitatively, whereas the fullerene is consumed insignificantly during the electrolysis, though the electrolysis is carried out at its reduction potentials. Obviously, mediated reduction of Au(I) to Au(0) occurs (Scheme 1). The metal that is generated is stabilized in the solution, so it is not deposited on the electrode. The UV-visible spectrum of the solution after the electrolysis differs considerably from the spectrum of the starting solution: along with the fullerene absorption bands, absorption in all the visible spectrum region is also observed (Figure 2c).

The metal is not deposited by centrifugation (15 000 rpm, 1 h) of the resulting homogeneous solution, either. Therefore, in order to study it by SEM, HR TEM and XRPD methods, the solvent was evaporated in vacuo, then the residue was successively washed with water, toluene and ethanol to remove the supporting electrolyte, fullerene, and residual amounts of DMF and DCB (see Experimental), and dispersed in ethanol. It is interesting that only a small amount of fullerene was transferred to the solution upon dispersing of the resulting deposit by sonication in toluene followed by centrifugation, and the toluene

Figure 4. Pictures of 1.3 mM C_{60} + 1.0 mM AuCl solution in DCB-DMF (2:1)/0.1 M Bu_4NCl medium before (left) and after (right) the electrolysis at −0.4 V (Q = 1.0 F with respect to AuCl).

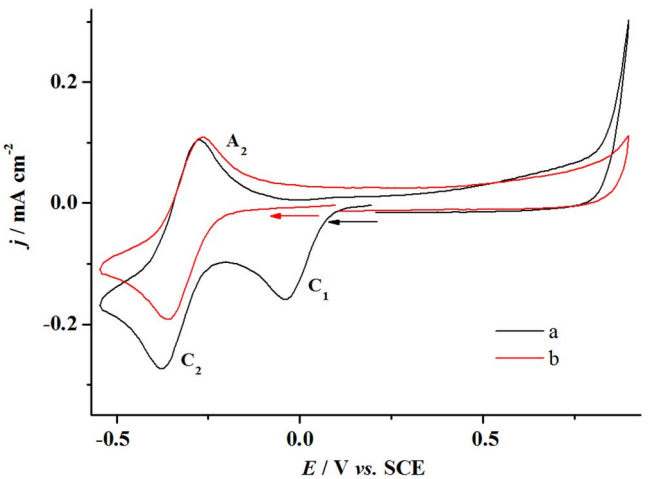

Figure 5. CV curves of the 1.3 mM C_{60} + 1.0 mM AuCl system before (a) and after the preparative reduction at −0.40 B (Q = 1.0 F with respect to AuCl) (b) in DCB-DMF (2:1)/0.1 M Bu_4NCl medium. $\nu = 100$ mV/s.

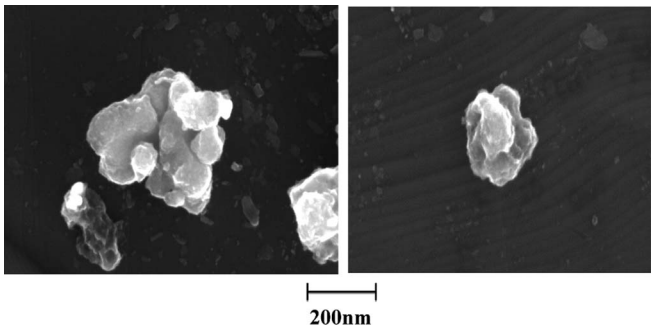

Figure 6. A SEM image of the Au-NPs/C_{60} nanocomposite.

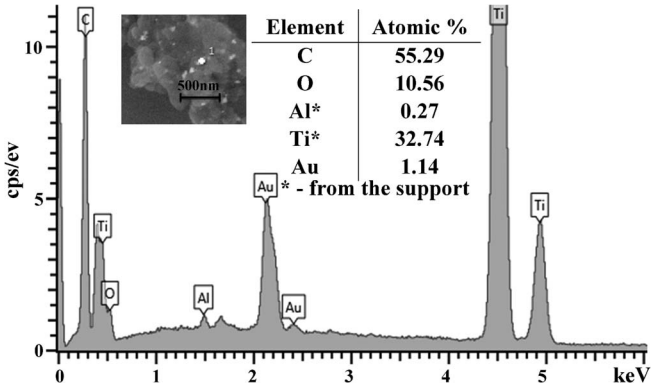

Figure 7. Energy-dispersive spectrum of the cross-marked region of the Au-NPs/C_{60} nanocomposite applied on a titanium substrate.

solution remained nearly colorless. We explain this fact as follows: the deposit contains nearly no free fullerene as it is completely bound with metal particles, and this composite containing C_{60} and Au(0) in ~1:1 ratio is insoluble in toluene.

A SEM image of the composite (Figure 6) shows large nanoparticles with diverse shapes and sizes, with inclusions of smaller nanoparticles. It follows from the energy-dispersive spectra that the included nanoparticles contain Au and carbon (Figure 7), whereas the majority of the large nanoparticles contain no gold and consist almost completely of carbon (Figure 8). Thus, the composite obtained is a nanocomposite of Au-NPs with C_{60} fullerene.

It becomes clear from the HR TEM image (Figure 9) and the energy-dispersive spectrum that the nanocomposite has the form of separate gold nanoparticles with diverse shapes and a mean size of $\sim 27 \pm 14$ nm, as well as larger nanoaggregates with various sizes and shapes, isolated in a fullerene matrix.

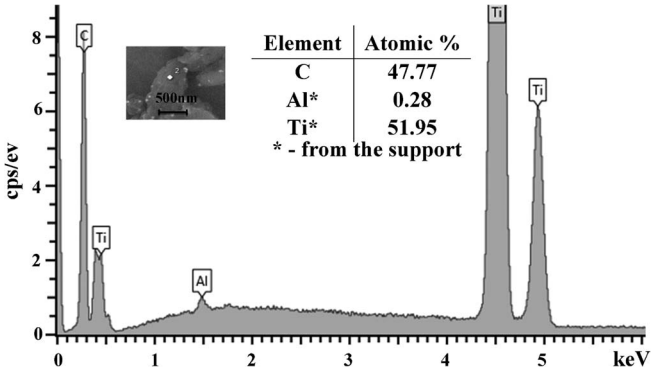

Figure 8. Energy-dispersive spectrum of the cross-marked region of the Au-NPs/C_{60} nanocomposite applied on a titanium substrate.

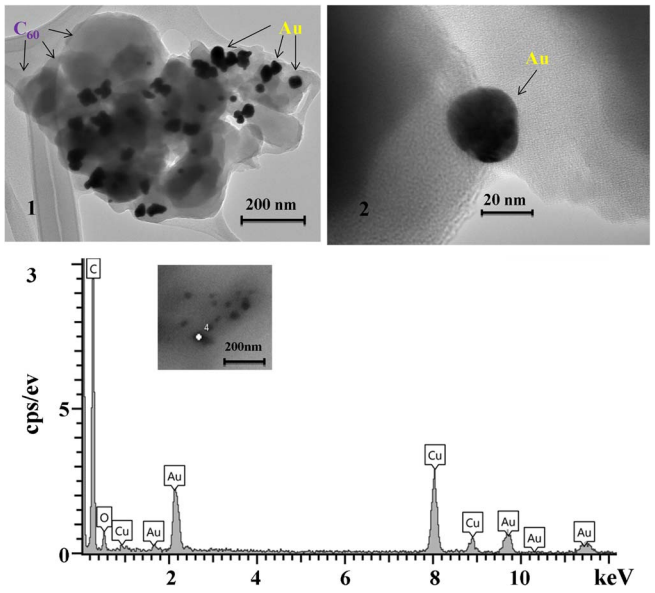

Figure 9. A HR TEM image (a, b) and an energy-dispersive spectrum from the cross-marked region (c) of the Au-NPs/C_{60} nanocomposite applied on a copper mesh with a formvar/carbon substrate.

As it was confirmed by XRPD analysis (Figure 10), the main interference peaks correspond to crystalline gold (code no. 00-004-0784 in the PDF database, the corresponding peak positions are shown by red vertical lines in the picture). The diffuse nature of the majority of the diffraction peaks suggest very small linear dimensions of the gold crystallites, i.e., it is nanostructured. The mean dimensions of the gold crystallites calculated from the interference peak widths are in the range of 9–14 nm. Furthermore, the sample also contains a small amount of another crystalline compound. Assuming that, based on the data obtained, the crystalline component may consist of C_{60} fullerene, we performed a search on the difference peaks in the X-ray diffraction pattern in the PDF-2 data base. It gave a suitable compound, namely, the hexagonal form of crystalline fullerene C_{60} – Carbon C_{60}, code no. 00-047-0787 (the positions of the diffraction peaks are shown as green lines in Figure 10). Thus, deposition of the starting suspension gave a few crystalline components, namely, gold and C_{60} fullerene.

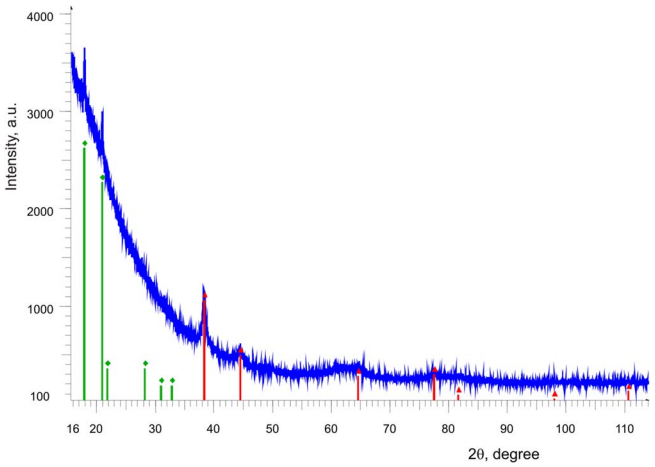

Figure 10. A fragment of the experimental diffraction patterns of the Au-NP/C_{60} nanocomposite without background subtraction. Red vertical lines show the positions of the interference peaks corresponding to crystalline gold – gold, syn., code no. 00-004-0784 in the PDF database; green vertical lines correspond to the interference peaks of hexagonal form of crystalline fullerene C_{60} – Carbon C_{60}, code no. 00-047-0787 in the PDF database.

An estimate of the crystallite dimensions for the latter based on the half-widths of the reflexes gave dimensions that were much larger than those of gold nanoparticles, *viz.*, ~68 nm. It may not be excluded here that the fullerene can form not only individual crystals but also, for instance, be involved in complexation and undergo crystallization with gold or with other components of the system. Taking into account that unit cells with similar parameters are characteristic of many such crystal solvates and co-crystals of fullerene (e.g., in cubic crystalline form of potassium mercury fullerene $C_{60}HgK_3$, code no. 00-049-1903, the peak positions in the X-ray diffraction pattern are very similar to those observed in the experiment), it is hard to estimate whether they are present from the X-ray diffraction pattern that we obtained experimentally. However, this assumption may be supported by the observation made during purification of the sample studied. While the pure fullerene is very well soluble in toluene, washing this sample with toluene did not result in fullerene "wash-out" from it, as the diffraction experiment confirms. At least, this observation requires a special study that we are going to perform shortly.

Conclusions

Thus, C_{60} fullerene mediated electroreduction of Au(I) at potentials of the $C_{60}/C_{60}^{\bullet-}$ redox couple allowed us to perform the electrosynthesis of an AuNP/C_{60} nanocomposite in DCB-DMF (2:1)/0.1 M Bu_4NCl medium. The nanocomposite consists of separate gold nanoparticles, with various shapes and a mean size of ~27 ± 14 nm, as well as larger nanoaggregates of such particles, isolated in a fullerene matrix. The mean size of the metal crystallites is 9–14 nm. The electrolysis occurs efficiently, and Au(I) is quantitatively reduced to Au(0) upon consumption of the theoretical amount of electricity. The resulting metal nanoparticles and the nanocomposite are not deposited on the electrode and are completely stabilized in the solution bulk. This result opens new prospects for the application of electrochemical reactions of fullerenes and their diverse derivatives not only in the mediated reduction of metal ions (complexes) and electrosynthesis of metal nanoparticles in solution bulk, but also for the preparation of nanocomposites containing nanoparticles of various metals in matrices of fullerenes and their derivatives. Composites of this kind are of certain practical interest ranging from sensors and photovoltaic cells to nanostructured devices for advanced electronic applications.[57]

Acknowledgments

The authors acknowledge the financial support from RSF (grant no. 14-23-00016).

References

1. R. E. Haufler, J. Conceicao, L. P. F. Chibante, Y. Chai, N. E. Byrne, S. Flanagan, M. M. Haley, S. C. O'Brien, C. Pan, Z. Xiao, W. E. Billups, M. A. Ciufolini, R. H. Hauge, J. L. Margrave, L. J. Wilson, R. F. Curl, and R. E. Smalley, *J. Phys. Chem.*, **94**, 8634 (1990).
2. L. Echegoyen, F. Diederich, and L. E. Echegoyen, in *Electrochemistry of Fullerenes / Fullerenes: Chemistry, Physics, and Technology*, Chapter 1, pp. 1, ed. K. M. Kadish and R. S. Ruoff, Lohn Wiley & Sons, Inc. (2000).
3. Q. Xie, E. Perez-Cordero, and L. Echegoyen, *J. Am. Chem. Soc.*, **114**, 3978 (1992).
4. Y. Ohsawa and T. Saji, *J. Chem. Soc., Chem. Commun.*, 781 (1992).
5. F. Zhou, C. Jeboulet, and A. J. Bard, *J. Am. Chem. Soc.*, **114**, 11004 (1992).
6. V. V. Yanilkin, *Electrochemistry of Fullerenes in Electrochemistry of organic compounds at the beginning of the XXI century*, pp. 178, ed. V. P. Gultiay, A. G. Krivenko, and A. P. Tomilov, Sputnik Inc, Moskau (2008).
7. I. A. Nuretdinov, V. P. Gubskaya, V. V. Yanilkin, V. I. Morozov, V. V. Zverev, A. V. Il'yasov, G. M. Fazleeva, and N. V. Nastapova, *Russ. Chem. Bull.*, **50**, 607 (2001).
8. I. A. Nuretdinov, V. V. Yanilkin, V. I. Morozov, V. P. Gubskaya, V. V. Zverev, N. V. Nastapova, and G. M. Fazleeva, *Russ. Chem. Bull.*, **51**, 263 (2002).
9. V. V. Yanilkin, N. V. Nastapova, V. P. Gubskaya, V. I. Morozov, L. Sh. Berezhnaya, and I. A. Nuretdinov, *Russ. Chem. Bull.*, **51**, 72 (2002).
10. V. V. Yanilkin, V. P. Gubskaya, V. I. Morozov, N. V. Nastapova, V. V. Zverev, E. A. Berdnikov, L. Sh. Berezhnaya, and I. A. Nuretdinov, *Russ. J. Electrochem.*, **39**, 1147 (2003).
11. T. Fuchigami, M. Kasuga, and A. Konno, *J. Electroanal. Chem.*, **411**, 115 (1996).
12. Y. Huang and D. D. M. Wayner, *J. Am. Chem. Soc.*, **115**, 367 (1993).
13. F. D'Souza, J.-p. Choi, Y.-Y. Hsick, K. Skriver, and W. Kutner, *J. Phys. Chem. B*, **102**, 212 (1998).
14. F. D'Souza, J.-p. Choi, and W. Kutner, *J. Phys. Chem. B*, **102**, 4247 (1998).
15. F. D'Souza, J.-p. Choi, and W. Kutner, *J. Phys. Chem. B*, **103**, 2892 (1999).
16. B. S. Sherigara, W. Kutner, and F. D'Souza, *Electroanalysis*, **15**, 753 (2003).
17. M. X. Li, M. Xu, N. Li, Z. Gu, and X. Zhou, *J. Phys. Chem. B*, **106**, 4197 (2002).
18. T. Liu, M. Li, N. Li, Z. Shi, Z. Gu, and X. Zhou, *Electrochim. Acta*, **45**, 2743 (2000).
19. T. Liu, M. Li, N. Li, Z. Gu, and X. Zhou, *Electrochim. Acta*, **45**, 4457 (2000).
20. M. Li, Y. Gao, N. Li, Z. Shi, Z. Gu, and X. Zhou, *Electroanalysis*, **13**, 1253 (2001).
21. M.-X. Li, N.-Q. Li, Z.-N. Gu, X.-H. Zhou, Y.-L. Sun, and Y.-Q. Wu, *Anal. Chim. Acta*, **356**, 225 (1997).
22. M. X. Li, N. Q. Li, Z. N. Gu, X. H. Zhou, Y. I. Sun, and Y. Q. Wu, *Microchem. J.*, **61**, 32 (1999).
23. H. Qian, J. Ye, and L. Jin, *Anal. Lett.*, **30**, 367 (1997).
24. H. Luo, N. Li, Z. Shi, Z. Gu, and X. Zhou, *Microchem. J.*, **65**, 17 (2000).
25. V. V. Yanilkin, A. V. Toropchina, V. I. Morozov, N. V. Nastapova, V. P. Gubskaya, F. G. Sibgatullina, N. M. Azancheev, Yu. Ya. Efremov, and I. A. Nuretdinov, *Electrochim. Acta*, **50**, 1005 (2004).
26. Z.-L. Shi, Y.-P. Mao, W. Tong, and L. T. Jin, *Chinese J. Chem.*, **12**, 117 (1994).
27. T. Liu, M. X. Li, N. Q. Li, Z. J. Shi, Z. N. Gu, and X. H. Zhou, *Talanta*, **50**, 1299 (2000).
28. A. D. Pomogaylo, A. S. Rosenberg, and I. E. Uflyand, *Metal nanoparticles in polymers*, Khimia, Moscow (2002).
29. V. I. Roldughin, *Russ. Chem. Rev.*, **69**, 821 (2000).
30. M. C. Daniel and D. Astruc, *Chem. Rev.*, **104**, 293 (2004).
31. I. P. Suzdalev, *Nanotechnology. Physicochemistry of nanoclusters, nanostructures and nanomaterials*, KomKniga, Moscow (2006).
32. V. V. Volkov, T. A. Kravchenko, and V. I. Roldughin, *Russ. Chem. Rev.*, **82**, 465 (2013).
33. L. A. Dykman and V. A. Bogatyrev, *Russ. Chem. Rev.*, **76**, 181 (2007).
34. B. I. Kharisov, O. V. Kharissova, and U. Ortiz-Mendez, *Handbook of less-common nanostructures*, CRC Press, Taylor & Francis Group, Boca Raton, 2012.
35. V. V. Yanilkin, G. R. Nasybullina, A. Y. Ziganshina, I. R. Nizamiev, M. K. Kadirov, D. E. Korshin, and A. I. Konovalov, *Mendeleev Commun.*, **24**, 108 (2014).
36. V. V. Yanilkin, G. R. Nasybullina, E. D. Sultanova, A. Y. Ziganshina, and A. I. Konovalov, *Russ. Chem. Bull.*, **63**, 1409 (2014).
37. V. V. Yanilkin, N. V. Nastapova, G. R. Nasretdinova, R. K. Mukhitova, A. Y. Ziganshina, I. R. Nizameev, and M. K. Kadirov, *Russ. J. Electrochem.*, **51**, 951 (2015).
38. S. Fedorenko, M. Jilkin, N. Nastapova, V. Yanilkin, O. Bochkova, V. Buriliov, I. Nizameev, G. Nasretdinova, M. Kadirov, A. Mustafina, and Y. Budnikova, *Colloids Surf. A Physicochem. Eng. Asp.*, **486**, 185 (2015).
39. V. V. Yanilkin, N. V. Nastapova, E. D. Sultanova, G. R. Nasretdinova, R. K. Mukhitova, A. Y. Ziganshina, I. R. Nizameev, and M. K. Kadirov, *Russ. Chem. Bull.*, **1**, 125 (2016).
40. G. R. Nasretdinova, Y. N. Osin, A. T. Gubaidullin, and V. V. Yanilkin, *J. Electrochem. Soc.*, **163**, G99 (2016).
41. G. R. Nasretdinova, R. R. Fazleeva, R. K. Mukhitova, I. R. Nizameev, M. K. Kadirov, A. Y. Ziganshina, and V. V. Yanilkin, *Electrochem. Commun.*, **50**, 69 (2015).
42. G. R. Nasretdinova, R. R. Fazleeva, R. K. Mukhitova, I. R. Nizameev, M. K. Kadirov, A. Y. Ziganshina, and V. V. Yanilkin, *Russ. J. Electrochem.*, **51**, 1029 (2015).
43. V. V. Yanilkin, N. V. Nastapova, G. R. Nasretdinova, R. R. Fazleeva, A. V Toropchina, and Y. N. Osin, *Electrochem. Commun.*, **59**, 60 (2015).
44. V. V. Yanilkin, R. R. Fazleeva, G. R. Nasretdinova, N. V. Nastapova, and Y. N. Osin, *Butlerov commun.*, **46**, 128 (2016).
45. V. V. Yanilkin, G. R. Nasretdinova, Y. N. Osin, and V. V. Salnikov, *Electrochim. Acta*, **168**, 82 (2015).
46. V. V. Yanilkin, N. V. Nastapova, G. R. Nasretdinova, S. V. Fedorenko, M. E. Jilkin, A. R. Mustafina, A. T. Gubaidullin, and Y. N. Osin, *RSC Adv.*, **6**, 1851 (2016).
47. V. V. Yanilkin, N. V. Nastapova, G. R. Nasretdinova, R. R. Fazleeva, and Y. N. Osin, *Electrochem. Commun.*, **69**, 36 (2016).
48. V. Saez and T. J. Mason, *Molecules*, **14**, 4284 (2009).
49. J. Zhu, S. Liu, O. Palchik, Yu. Koltypin, and A. Gedanken, *Langmuir*, **16**, 6396 (2000).
50. J. Reisse, T. Caulier, C. Deckerkheer, O. Fabre, J. Vandercammen, J. L. Delplancke, and R. Winand, *Ultrason. Sonochem.*, **3**, 147 (1996).
51. M. T. Reetz and W. Helbig, *J. Am. Chem. Soc.*, **116**, 7401 (1994).
52. J. A. Becker, R. Scha¨fer, R. Festag,W. Ruland, J. H. Wendorff, J. Pebler, S. A. Quaiser, W. Helbig, and M. T. Reetz, *J. Chem. Phys.*, **103**, 2520 (1995).
53. M. T. Reetz, S. A. Quaiser, and C. Merk, *Chem. Ber.*, **129**, 741 (1996).
54. M. T. Reetz, W. Helbig, S. A. Quaiser, U. Stimming, N. Breuer, and R. Vogel, *Science*, **267**, 367 (1995).
55. M. T. Reetz, M. Winter, R. Breinbauer, T. Thurn-Albrecht, and W. Vogel, *Chem. Eur. J.*, **7**, 1084 (2001).
56. DIFFRAC Plus Evaluation package EVA, Version 11, User's Manual, Bruker AXS, Karlsruhe, Germany, 258 p. (2005).
57. D. Bonifazi, O. Engerc, and F. Diederich, *Chem. Soc. Rev.*, **36**, 390 (2007).